Plutonium – Uranium – Zirconium

Volodymyr Ivanchenko, Tatiana Pryadko

Introduction

Pu-U-Zr system offers potential fuel materials for liquid-metal fast breeder reactor. Their compatibility with Type-304 stainless steel at temperatures up to 800°C makes them particularly valuable for this purpose. The applicability of particular Pu-U-Zr alloy compositions as fuel materials depends partially on properties related to the phase equilibria in the system. Furthermore, the temperatures of liquidus and solidus are important in assessing the possibility of fuel melting under abnormal reactor conditions. [1966Far1] reported results, obtained in Argonne National Laboratory on the study of phase relations in the U-12.9Pu-22.5Zr (at.%) alloy in temperature interval from 25°C to melting point. [1968Tuc] presented the (γU,εPu,βZr) solid solution surface. [1968Far1] and [1968Far4] reported results of phase equilibrium studies conducted at Mound Laboratory. The liquidus and solidus surfaces of the ternary system are known at high Pu concentrations showing that additions of Zr markedly increase the solidus and liquidus temperatures. Extensive studies were made by [1970Obo] presenting isothermal sections at 700, 670, 660, 650, 640, 595, 580, 550, and 500°C. [1988Lei] attempted to construct solidus and liquidus surfaces employing a state of the art approach that couples thermodynamic calculation with experimental determination of solidus and liquidus temperatures, in this case for three selected alloys. For the alloy compositions close to binary edges of the ternary diagram the calculated results agreed reasonably well with measured values. Using the experimental results of [1970Obo], [1999Kur] performed another thermodynamic assessment of the Pu-U-Zr system with reasonable agreement between calculated and experimental data. The publication of [2005Nak] shows that the Pu-U-Zr calculations by [1999Kur] can be applied to analyze the multicomponent interdiffusion zones of the metal fuel and the iron-based cladding.
[1965Far] reported the thermal expansion coefficient measured on U-14Pu-30Zr (at.%) alloys. Thermodynamic properties of U-12.2Pu-21.8Zr (at.%) alloy were presented by [1967Far2].
The information available on phase relations, structure and thermodynamic studies is summarized in Table 1.

Binary Systems

There are more than one version for the Pu-U and Pu-Zr phase diagrams. The first assessment of the Pu-U system based on experiments was presented by [1989Pet] and redrawn by [Mas2]. Later, [1991Lei] performed a thermodynamic assessments of this system. The main discrepancies between the calculated and the experimentally constructed phase diagram consists in the appearance of a maximum on the η/(η+ζ) phase border, that was in a serious contradiction with experimental results of thermal analysis presented by [1989Pet], which show the absence of a maximum. Some later [1999Kur] repeated the thermodynamic assessment of the Pu-U system and found a maximum too, at lower temperatures. But new problems arose from inconsistencies between the experimentally constructed and calculated slopes of the phase boundaries (αU) / (αU)+ζ / ζ. For these reasons here the Pu-U system is accepted as constructed by [1989Pet]. The Pu-Zr phase diagram was accepted in accordance with [1993Oka], who took into account results of [1967Lau] and [1992Suz] stabilizing the κ-phase by oxygen. The U-Zr phase diagram is accepted as reported in [Mas2].

Solid Phases

No ternary phases are formed in the Pu-U-Zr system. The crystal structures of unary and binary phases are presented in Table 2. Since all the phases in the ternary system are common to one of the limiting binary systems, the same nomenclature has been used to identify both the binary and ternary system phases in accordance with [1970Obo]. Phase designations used in the present evaluation are as follows: γ is the *a* body-centred-cubic allotropic modification of U that has complete solid solubility with bcc (εPu) and bcc

(βZr). γ_1 is the U rich, γ_2 the Zr rich modification of γ participating in the monotectoid reaction in the U-Zr system. (αU) and (βU) are orthorhombic and tetragonal allotropic modifications of U that dissolve up to 15 and 20 at.% Pu, respectively, but have limited solid solubility of Zr. η is a high-temperature intermediate Pu-U phase that is believed to be tetragonal and has limited solubility for Zr. ζ is a complex cubic U-Pu intermediate phase that dissolves up to 5 at.% Zr. δ stands for a hexagonal intermediate phase in the U-Zr binary system that occurs approximately at the composition UZr_2 and has extensive solubility for Pu. (δPu) is the fcc allotropic modification of Pu that has extensive solid solubility for Zr but very limited solubility for U.

Invariant Equilibria

The scheme of solid-state reactions is given in Fig. 1, based on [1970Obo] but modified in the peritectoid reaction (αU) + (γU,Zr) ⇌ (δU,Zr) according to the accepted U-Zr binary system.

Liquidus, Solidus and Solvus Surfaces

Liquidus and solidus temperatures in the Pu corner are presented in Fig. 2 based on work by [1968Far1] and [1968Far4] that was conducted at Mound Laboratory and again slightly corrected in accordance with the accepted Pu-Zr binary phase diagram. In the part of reaction scheme including δ, γ, (αZr) and ζ phases the (εPu,γU,βZr) solid solution surface presented by [1968Tuc] was neglected as it is inconsistent with the results of [1970Obo].

Isothermal Sections

Isothermal sections at 700, 670, 660, 650, 640, 595, 580, 550 and 500°C experimentally constructed by [1970Obo] are given in Figs. 3 to 11. These section were corrected according to the accepted binary systems. Isothermal sections at 670 (Fig. 4), 650 (Fig. 6), 595, 580 and 550°C (Figs. 8 to 10) correspond to the temperatures of the nonvariant reactions P, U_1, U_2, U_3 and U_4. The related four-phase planes are included in the figures.

Thermodynamics

The limited number of experimental data on thermodynamic properties is listed in Table 3 and Table 4.

Notes on Materials Properties and Applications

Thermal expansion coefficient α of the U-12.9Pu-30Zr (at.%) alloy is $18.2 \cdot 10^{-6}$ $°C^{-1}$ in the temperature interval 25 to 596°C. During the phase transformation, in the interval of 596 to 665°C $\Delta l = 0.58\%$ and after the transformation is completed, in the temperature interval of 665 to 950°C, $\alpha = 22.3 \cdot 10^{-6}$ $°C^{-1}$ [1965Far]. [1966Far1] reported data on thermal conductivity measured on U-15Pu-1Zr (at.%) alloys at 100 to 900°C. Thermal conductivity of the alloy U-15Pu-15Zr (at.%) is K = 0.111 watt·((cm)(°C))$^{-1}$ at 100°C and rises to 0.301 watt·((cm)(°C))$^{-1}$ at 900°C. For U-15Pu-25Zr (at.%) K equals 0.0021 watt·((cm)(°C))$^{-1}$ at 100°C and 0.260 watt·((cm)(°C))$^{-1}$ at 900°C. Mechanical properties of some Pu-U-Zr alloys [1968Far1] are presented in Tables 6 to 8.
[1967Bec] studied the performance of advanced Pu-U-Zr alloy fuel element under fast reactor conditions. Information about investigations of the Pu-U-Zr materials properties is summarized in Table 5.

Miscellaneous

Various ceramics have been evaluated to find a suitable container material for melting and casting U-Zr and Pu-U-Zr alloys, and most of them proved to be totally inadequate. To date the U - 10Zr (mass%) alloy melted in Gd_2O_3 crucibles has come out with the smallest pickup of oxygen. [1969Far], basing on the results obtained at Los Alamos Scientific Laboratory, reported, that the most promising crucible coating appears to be colloidal suspension of Y_2O_3 spread onto the crucible surface. Very good results were obtained, when water-cooled metallic crucible were used. In this case a frozen alloy skin next to the crucible prevents

impurity pickup from the crucible. The technological route used in Argonne National laboratory included the production of U base and Pu base master alloys alloyed with Zr, using thoria, zirconia or magnesia crucibles coated with yttria. Alloy chunks were melted in yttria-coated graphite crucible using induction furnace. Pins were produced by injection casting into large-L/D-ratio Vycor mold [1978Hin].

The ultimate criteria for fuel pin design is the overall integrity up to the planned life time or target burnup of irradiation. Here, burnup is defined by the fraction of total heavy metal constituents (U+Pu), which have undergone fission and, hence, transferred thermal power to the sodium reactor coolant medium flowing around the pins. Achievement of burnup near 15 at.% is desirable for large scale commercialization of liquid-metal reactors (LMR). The fuel itself is a solid cylinder which has been injection-casted into quartz molds and loaded into the cladding jacket with no prior thermomechanical treatment required. The as cast density of these alloys is ~15.8 $g \cdot cm^{-3}$. Sodium fills annulus around the slug and provides the high conductivity heat path to the cladding prior to fuel slug swelling. The plenum space (initially filled with inert gas) above the fuel slug is provided to contain the large volume of stable fission gas (Xe/Kr) which is produced in these fuel slugs at a rate of ~16 cm^3 per percent burnup. The ends of the jacket are hermetically sealed with an automatic tungsten inert gas welder and a helical wire is welded in place to maintain pin spacing and mix coolant flow upward through the close-packed hexagonal pin bundle during irradiation [1990Pah]. Prior to making contact with the cladding tube, metallic alloy fuel swells rapidly due to its high fission-enhanced creep rate and irradiation growth. It has been determined that fission rate, temperature, and plutonium concentration influence the observed macroscopic swelling rate [1990Ger].

The key phenomena which are significant in controlling the fuel pin behavior and reliability are summarized in Table 9.

These swelling phenomena have been subject of many investigations.

It was shown, that U-14.4Pu-29.3Zr (at.%) alloy jacketed in a V - 20Ti (mass%) alloy and irradiated to burnups of 12.5% at 665°C elongated 3% at 4.2% burnup. No further change in length was observed throughout the remaining irradiation. The fission-gas pores were interconnected and the fuel cracked radially [1967Far1]. Density measurements of annual sections of fuels after burnups of 4.6 at.% show that the least-dense fuel is consistently found in the middle zone and the most-dense fuel is in the center zone [1968Far3]. Analyses of irradiated U-15Pu-10Zr (mass%) (U-12.2Pu-21.8Zr (at.%)) showed that considerable amounts of Zr and Tc migrated from the middle of the three annular zones noted in these fuel elements. There was also evidence of some depletion of fission products in the middle zone, and changes in the original alloy composition [1968Far2, 1969Rhu]. The fuel restructuring has been traced carefully as a function of fuel burnup by [1990Por]. The results indicated that the porosity distributions would lead to significant changes in the fuel operating temperature. Concurrent observations concerning composition redistribution indicated that a significant redistribution of constituents proceeded the developing of porosity. [1969Smi] shortly considered the problems concerned with fission products release from Pu-U-Zr ternary alloy fuel element.

Constituent redistribution in a metallic alloy fuel can occur by solid state diffusion under gradients of temperature and concentration. The redistribution is also influenced significantly by irradiation and phase transformation. As a result, an originally uniformly mixed alloy can change to an inhomogeneous alloy. Inhomogeneity in a metallic nuclear fuel alloy can cause phase transformations, solidus temperature change, and local change in the density of fissible atoms, which can alter the physical and mechanical properties of the alloy fuel affecting its behavior and performance. As it was shown by [2000Soh], the flux contributions by the gradients of U and Zr are similar in magnitude but have opposite signs. The U migration to the colder regions of the sample is driven by both gradients of temperature and Zr concentration. Similarly, the Zr migration to the hot end of the sample is driven by both gradients of temperature and U concentration. Pu-U-Zr metallic alloy fuel irradiated to the end-of-life burnup of 1.9 at.% exhibits three distinct phase regions. For a fuel composition of U-15.5Pu-21.9Zr (at.%), the center region was composed of γ (above 650°C), the intermediate region of γ+ζ (600-650°C), and the outer region of δ+ζ (500-600°C) phases [2004Kim]. Thermally activated constituent migration took place in the initially homogeneous fuel, and then, as the concentration gradient builds up, migration due to concentration gradients is followed.

Fuel/cladding chemical interaction involves the interdiffusion of fuel and cladding constituents at operating temperatures. Isothermal experiments at 650°C of U-21Pu-23Zr/HT9 and U-21Pu-23Zr/D9 (at.%) diffusion

couples were performed by [1996Kei] to assess the role of Ni on interdiffusion behavior. It was shown, that the number of observed phases and the diffusion zone size is higher for couples with negligible Ni (U-21Pu-23Zr/HT9) than for the couples with 16 mass% Ni (U-21Pu-23Zr/D9 (at.%)).
The interdiffusion is characterized by diffusion of Fe and Ni, when available as cladding constituents into the fuel, with corresponding diffusion of lantanide fission products (La, Ce, Nd, Sm, Pr) into cladding [1990Pah]. At minor degrees of interaction, metallography examination often doe not reveal the area of interaction in the fuel. The interaction in the cladding, however follows a very defined interaction front, leaving a layer of cladding which contains nearly 20 mass% of the lantanides [1990Pah]. Rare earth with the Fe and Ni constituents of stainless steel interact to form compounds that melt below 1000 K. U preferentially interacts with Fe, whereas the rare earth interact with Ni. In the absence of U, Fe interact with the rare earths and in this case the formed Fe and Ni interaction compounds melt at a temperature around 890 K [1994Sar].
To decrease the fuel/cladding interaction a Zr coating may be used. Zr-sheet fuel elements irradiated to 2 at.% burnup exhibit significantly less axial growth that standard-cast fuel elements (1.3 to 1.8 versus 4.9 to 8.1%). A 0.2 mm thick Zr sheet around U-20.5Pu-3Zr (mass%) fuel alloy does not provide a reliable barrier against fuel/cladding chemical interaction under irradiation [1993Cra].
[1966Huf] showed, that anion exchange-partition chromatography can be applied to the trace the impurity in ternary Pu-U-Zr alloys.
The results of the postirradiation examination of U-14.4Pu-29.3Zr (at.%) alloy performed in Argonne National Laboratory were presented by [1967Far1, 1968Far2, 1968Far3, 1968Far4]. Emphasis at Argonne was centred upon the U-15Pu-10Zr (mass%) (U-12.2Pu-21.8Zr (at.%)) and U-15Pu-15Zr (mass%) (U-11.5Pu-30.7Zr (at.%)) alloys. They were tested as the most promising alloys for fast breeder application [1969Fac]. Results of development of alloying and casting techniques, fabrication of test fuel elements, fuel element performance during irradiation and solid state reactions are shortly reported by [1968Far4, 1969Far, 1977Lam, 1978Hin]. Microstructural changing in fuel, redistribution of components and nucleation and growth of the Xe/Kr fission gas bulbs were analyzed by [1988Lah, 1988Hof, 1988Pah]. An analysis of fission gas release and induced swelling in steady state irradiated Pu-U-Zr metal fuels was performed by [1989Ste] using computer modelling. Irradiation and fission related phenomena in metallic Pu-U-Zr fuels resulted in fuel swelling and in redistribution of the constituents, as studied by [1990Por]. The results of experimental studies of Pu-U-Zr fast reactor fuel pins irradiated to >15 at.% burnup, including fission gas retention & release as well as fuel/cladding chemical interaction have been reported by [1990Pah]. A model for the constituents' migration behavior in Pu-U-Zr metallic fast reactor fuel has been proposed by [1993Ish]. The model can predict the experimentally observed radial three-zone structure and the zirconium and uranium redistribution, however the predicted radial location of zirconium-depleted middle zone disagreed with the experimental result. The swelling mechanisms in the (αU) phase has been modelled by [1993Res]. The results of this study demonstrate that the relatively long incubation times characteristic for the Integral Fast Reactor swelling and the gas release can be understood in terms of a reduced gas-bubble nucleation rate at the α/δ phase boundaries. [1993Cra] reported the behavior of Pu-U-Zr fuel cast in zirconium moulds with relation to chemical interaction of fuel and cladding. Redistribution behavior of lanthanide fission products as well as their chemical interaction with cladding have been reported by [1990Pah, 1994Kur, 1994Sar]. [1996Kei] reported results from diffusion couples annealed at 650°C for 100 h between a Pu-U-Zr alloy and stainless steel, with and without Ni. Isothermal diffusion couple experiments were performed by [1997Pet] at 750°C and [1998Ale] at 800°C to investigate diffusion phenomena in body-centred cubic Pu-U-Zr alloys. Microstructural development and constituent redistribution were investigated by [2000Soh] in rods of a 62U-15.5Pu-21.9Zr (at.%) annealed at a temperature gradient of 220°C·cm^{-1}. Appreciable diffusional interaction were identified between Zr and U. An enrichment of Zr with concurrent depletion of U was observed on the hot-end side (~ 740°C). These results were confirmed by [2004Kim], who measured the postirradiation redistribution profiles of the fuel components. The interdiffusion fluxes of Zr, U and Pu in Pu-U-Zr fuel were calculated.
The metallic fuel anode in the molten salt electro-refining during pyrometallurgical reprocessing was modelled by [2005Iiz] based on the findings from the anodic dissolution tests of Pu-U-Zr ternary alloys.

References

[1965Far] Farkas, M.S., Storhok, V.W., Pardue, W.M., Martin, R.L., Stoltz, D.L., Kizer, D.E., Veigel, N.D., Townley, C.W., Barnes, R.H., Wright, T.R., Chubb, W., Speidel, E.O., Rough, F.A., "Fuel and Fertile Materials - Uranium Metal and Alloys - Plutonium - Thorium Compounds - Metal-Ceramic Fuels - Coated-Particle Fuel Materials - Uranium Oxides - Uranium and Thorium Carbides, Nitrides, and Phosphides - Basic Studies of Irradiation Effects", *Reactor Mater.*, **8**(3), 119-134 (1965) (Assessment, Mechan. Prop., Phase Diagram, Phase Relations, Phys. Prop., Transport Phenomena, 70)

[1966Far1] Farkas, M.S., Storhok, V.W., Pardue, W.M., Smith, R.A., Veigel, N.D., Miller, N.E., Wright, T.R., Barnes, R.H., Chubb, W., Lemmon, A.W., Berry, W.E., Rough, F.A., "Fuel and Fertile Materials - Uranium Metal and Alloys - Plutonium - Thorium - Metal-Ceramic Fuels - Coated-Particle Fuel Materials - Uranium and Thorium Oxides - Uranium Carbides, Nitrides, Phosphides, Sulfides and Arsenides - Fuel-Water Reactions", *Reactor Mater.*, **9**(3), 151-165 (1966) (Assessment, Electr. Prop., Mechan. Prop., Phys. Prop., Transport Phenomena, 77)

[1966Far2] Farkas, M.S., Storhok, V.W., Pardue, W.M., Martin, R.L., Smith, R.A., Stoltz, D.L., Veigel, N.D., Miller, N.E., Wright, T.R., Lemmon, A.W., Acuncius, D.S., Chubb, W., Rough, F.A., "Fuel and Fertile Materials - Uranium Metal and Alloys - Plutonium - Plutonium Compounds - Thorium - Metal-Ceramic Fuels - Coated-Particle Fuels - Uranium Oxide Fuels - Uranium and Thorium Carbides, Nitrides, Sulfides, and Phosphides - Basic Studies of Irradiation", *Reactor Mater.*, **9**(2), 73-90 (1966) (Assessment, Crys. Structure, Phase Diagram, Phase Relations, Phys. Prop., Thermodyn., 74)

[1966Huf] Huff, E.A., Kulpa, S.J., "Trace Impurity Analysis of Plutonium-Uranium-Zirconium Alloys by Anion Exchange-Partition Chromatography", *Anal. Chem.*, **38**(7), 939-940 (1966) (Phys. Prop., 4)

[1967Bec] Beck, W.N., Brown, F.L., Koprowski, B.J., Kittel, J.H., "Perfomance of Advanced U-Pu-Zr Alloy Fuel Elements Under Fast-Reactor Conditions", *Trans. Amer. Nucl. Soc.*, **10**(1), 106-107 (1967) (Abstract, Transport Phenomena, 2)

[1967Far1] Farkas, M.S., Storhok, V.W., Askey, D.F., Pardue, W.M., Martin, R.L., Lozier, D.E., Veigel, N.D., Miller, N.E., Barnes, R.H., Chubb, W., Acuncius, D.S., Genco, J.M., Markworth, A.J., "Fuel and Fertile Materials - Uranium and Uranium Alloys - Plutonium - Thorium - Metal-Ceramic Fuels - Coated-Particle Fuels - Uranium and Thorium Oxide Fuels - Uranium Carbides, Nitrides, Phosphides and Sulfides - Fuel-Water Reactions - Basic Studies of Irradiation Effect", *Reactor Mater.*, **10**(3), 135-151 (1967) (Assessment, Phase Diagram, Phase Relations, Phys. Prop., 77)

[1967Far2] Farkas, M.S., Storhok, V.W., Pardue, W.M., Askey, D.F., Martin, R.L., Lozier, D.E., Smith, R.A., Veigel, N.D., Barnes, R.H., Wright, T.R., Chubb, W., Acuncius, D.S., Genco, J.M., Rough, F.A., "Fuel and Fertile Materials - Uranium Metal and Alloys - Plutonium - Thorium - Metal-Ceramic Fuels - Coated-Particle Fuels - Uranium and Thorium Oxides - Uranium Carbides, Nitrides, Phosphides and Sulfides - Fuel-Water Reactions - Basic Studies of Irradiaton Effect", *Reactor Mater.*, **10**(2), 69-82 (1967) (Assessment, Interface Phenomena, Phase Diagram, Phase Relations, Thermodyn., 73)

[1967Lau] Lauthier, J.C., Housseau, N., Van Craeynest, A., Calais, D., "Contribution to the Study of the Plutonium-Zirconium Phase Diagram" (in French), *J. Nucl. Mater.*, **23**, 313-319 (1967) (Phase Diagram)

[1968Tuc] Tucker, P.A., Etter, D.E., Gebhart, J.M., "Phase Study of Uranium-Plutonium-Zirconium Alloys", *Trans. Amer. Nucl. Soc.*, **11**, 99 (1968) (Abstract, Phase Relations, 2)

[1968Far1] Farkas, M.S., Daniel, N.E., Askey, D.F., Martin, R.L., Lozier, D.E., Barnes, R.H., Wright, T.R., Chubb, W., Lowder, J.T., Genco, J.M., Markworth, A.J., "Fuel and Fertile Materials - Uranium Metal and Alloys - Plutonium - Thorium - Metal-Ceramic Fuels - Uranium and Thorium Oxides - Carbide and Nitride Fuels - Fuel-Water Reactions - Basic

Studies of Irradiation Effects in Fuel Materials", *Reactor Mater.*, **10**(4), 203-216 (1968) (Crystal Structure, Experimental, Mechanical Properties, Phase Diagram, Phase Relations, Thermodynamics, Transport Phenomena, 66)

[1968Far2] Farkas, M.S., Daniel, N.E., Askey, D.F., Martin, R.L., Smith, J.T., Barnes, R.H., Wright, T.R., Chubb, W., Lowder, J.T., Genco, J.M., Berry, W.E., Markworth, A.J., "Fuel and Fertile Materials - Uranium and Uranium Alloys - Plutonium - Thorium - Metal-Ceramic Fuels - Uranium and Thorium Oxides - Carbide and Nitride Fuels - Fuel-Water Reactions - Corrosion Mechanisms of Fuel Alloys - Basic Studies of Irradiation Effect", *Reactor Mater.*, **11**(4), 205-219 (1968) (Assessment, Interface Phenomena, Mechan. Prop., Thermodyn., Transport Phenomena, 79)

[1968Far3] Farkas, M.S., Daniel, N.E., Askey, D.F., Martin, R.L., Lozier, D.E., Smith, R.A., Veigel, N.D., Barnes, R.H., Wright, T.R., Chubb, W., Markworth, A.J., "Fuel and Fertile Materials - Uranium Metal and Alloys - Plutonium - Thorium - Metal-Ceramic Fuels - Coated-Particle Fuels - Uranium and Thorium Oxides - Carbide and Nitride Fuels - Basic Studies of Irradiation Effects in Fuel Materials", *Reactor Mater.*, **11**(3), 145-156 (1968) (Assessment, Phase Diagram, Phase Relations, Transport Phenomena, 66)

[1968Far4] Farkas, M.S., Daniel, N.E., Askey, D.F., Martin, R.L., Veigel, N.D., Barnes, R.H., Wright, T.R., Chubb, W., Lowder, J.T., Genco, J.M., Markworth, A.J., "Fuel and Fertile Materials - Uranium and Uranium Alloys - Plutonium - Thorium - Metal-Ceramic Fuels - Uranium and Thorium Oxides - Uranium Carbides, Nitrides, Phosphides and Sulfides - Fuel-Water Reactions - Basic Studies of Irradiation Effects in Fuel Materials", *Reactor Mater.*, **11**(2), 81-92 (1968) (Assessment, Crys. Structure, Electr. Prop., Phase Diagram, Phase Relations, Thermodyn., Transport Phenomena, 61)

[1969Rhu] Rhude, H.V., Murphy, W.F., Natesh, R., "Irradiation Behavior of U-Pu-Zr Fuel Elements in EBR-II", *Trans. Amer. Nucl. Soc.*, **12**(2), 557-558 (1969) (Abstract, Transport Phenomena, 3)

[1969Smi] Smith, R.R., Ebersole, E.R., Fryer, R.M., Henault, P.B., "Fission Product Release from an Encapsulated U-Pu-Zr Ternary Alloy Fuel Element", *Trans. Amer. Nucl. Soc.*, **12**(1), 180 (1969) (Abstract, Transport Phenomena)

[1969Fac] Fackelmann, J.M., Askey, D.F., Houston, M.D., Martin, R.L., Smith, J.T., Smith, R.A., Barnes, R.H., Wright, T.R., Chubb, W., Lowder, J.T., Rosenberg, H.S., Berry, W.E., Markworth, A.J., "Fuel and Fertile Materials - Uranium Metal and Alloys - Plutonium - Thorium and Its Alloys - Metal-Ceramic Fuels - Uranium and Thorium Oxides - Uranium Carbide, Nitride and Sulfide Fuels - Fuel Reactions Following Loss-of-Coolant Accidents", *Reactor Mater.*, **12**(2), 73-88 (1969) (Assessment, Phase Diagram, Phase Relations, Phys. Prop., Thermodyn., 83)

[1969Far] Farkas, M.S., Koester, R.D., Askey, D.F., Houston, M.D., Martin, R.L., Smith, J.T., Smith, R.A., Veigel, N.D., Barnes, R.H., Wright, T.R., Chubb, W., Lowder, J.T., Markworth, A.J., "Fuel and Fertile Materials - Uranium and Uranium Alloys - Plutonium - Thorium - Metal-Ceramic Fuels - Coated-Particle Fuels - Uranium and Thorium Oxides - Carbide and Nitride Fuels - Basic Studies of Irradiation Effects in Fuel Materials", *Reactor Mater.*, **12**(1), 1-15 (1969) (Assessment, Phase Diagram, Phase Relations, Thermodyn., 76)

[1970Obo] O'Boyle, D.R., Dwight, A.E., "The Uranium-Plutonium-Zirconium Ternary Alloy System", *Nucl. Mater.*, **17**, 720-732 (1970) (Phase Diagram, Experimental, 17, #)

[1977Lam] Lam, P.S.K., Barthold, W.P., "An Assessment of the Breeding Potential of U-Pu-Zr Metal-Fueled 1200MW(e) LMFBRs", *Trans. Amer. Nucl. Soc.*, **27**, 753-754 (1977) (Assessment, 3)

[1978Hin] Hins, A.G., Kraft, D.A., Jelinek, H.F., "Remote Alloying and Casting of U-Pu-Zr Metal Fuel", *Trans. Amer. Nucl. Soc.*, **30**, 310-311 (1978) (Experimental, Phase Relations, 6)

[1988Lei] Leibowitz, L., Veleckis, E., Blomquist, R.A., Pelton, A.D., "Solidus and Liquidus Temperatures in the Uranium-Plutonium-Zirconium System", *J. Nucl. Mater.*, **154**(1), 145-153 (1988) (Phase Diagram, 30)

[1988Lah] Lahm, C.E., Porter, D.L., Pahl, R.G., "Fuel Constituent Redistribution During the Early Stages of U-Pu-Zr Irradiation", *J. Metals*, **40**(7), A86 (1988) (Abstract, 0)

[1988Hof] Hofman, G.L., Pahl, R.G., Lahm, C.E., Porter, D.L., "Swelling Behavior of U-Pu-Zr Fuel to High Burnup", *J. Metals*, **40**(7), A86 (1988) (Abstract, Transport Phenomena)

[1988Pah] Pahl, R.G., Lahm, C.E., Porter, D.L., Hofman, G.L., "Experimental Studies of U-Pu-Zr Fast Reactor Fuel Pins in EBR-II", *J. Metals*, **40**(7), A71 (1988) (Abstract, Phase Relations, 0)

[1989She] Sheldon, R.I., Peterson, D.E., "The U-Zr (Uranium-Zirconium) System", *Bull. Alloy Phase Diagrams*, **10**(2), 165-171 (1989) (Crys. Structure, Phase Relations, Phase Diagram, Thermodyn., Assessment, #, 33)

[1989Pet] Peterson, D.E., Foltyn, E.M., "The Pu-U (Plutonium-Uranium) System", *Bull. Alloy Phase Diagrams*, **10**(2), 160-164 (1989) (Crys. Structure, Phase Relations, Phase Diagram, Thermodyn., Assessment, #, 24)

[1989Ste] Steele, W.G., Wazzan, A.R., Okrent, D., "Steady-State Fission Gas Behavior in Uranium-Plutonium-Zirconium Metal Fuel Elements", *Nucl. Eng. Des.*, **113**(3), 289-295 (1989) (Theory, Phase Relations, 7)

[1990Por] Porter, D.L., Lahm, C.E., Pahl, R.G., "Fuel Constituent Redistribution during the Early Stages of U-Pu-Zr Irradiation", *Metall. Trans. A*, **21**(7), 1871-1876 (1990) (Phase Relations, Experimental, Transport Phenomena, 7)

[1990Pah] Pahl, R.G., Porter, D.L., Lahm, C.E., Hofman, G.L., "Experimental Studies of U-Pu-Zr Fast Reactor Fuel Pins in the Experimental Breeder Reactor-II", *Metall. Trans. A*, **21**(7), 1863-1870 (1990) (Phase Relations, Experimental, Transport Phenomena, 11)

[1990Ger] Gerard, L., Hofman, G.L., Pahl, R.G., Lahm, C.E., Porter, D.L., "Swelling Behavior of U-Pu-Zr Fuel", *Metall. Trans. A*, **21**(3), 517-528 (1990) (Phase Relations, Experimental, Transport Phenomena, 6)

[1991Lei] Leibowitz, L., Blomqusit, R.A., Pelton, A.D., "Thermodynamic Modeling of the Phase Equilibria of the Plutonium-Uranium System", *J. Nucl. Mater.*, **184**, 59-64 (1991) (Calculation, Thermodyn., 10)

[1992Suz] Suzuki, Y., Maeda, A., Ohmichi, T., "The Phase Diagram of Pu-Zr System in the Zr rich Region", *J. Alloys Compd.*, **182**(2), L9-L14 (1992) (Cryst. Structure, Experimental, Phase Diagram, 8)

[1993Ish] Ishida, M., Ogata, T., Kinoshita, M., "Constituent Migration Model for U-Pu-Zr Metallic Fast Reactor Fuel", *Nucl. Techn.*, **104**(1), 37-51 (1993) (Theory, Transport Phenomena, 19)

[1993Res] Rest, J., "Kinetics of Fission-Gas-Bubble-Nucleated Void Swelling of the α-Uranium Phase of Irradiated U-Zr and U-Pu-Zr Fuel", *J. Nucl. Mater.*, **207**, 192-204 (1993) (Calculation, Kinetics, Phys. Prop., 16)

[1993Cra] Crawford, D.C., Lahm, C.E., Tsai, H., Pahl, R.G., "Performance of U-Pu-Zr Fuel Cast Into Zirconium Molds", *J. Nucl. Mater.*, **204**, 157-164 (1993) (Experimental, Interface Phenomena, 11)

[1993Oka] Okamoto, H., "Pu-Zr (Plutonium-Zirconium)", *J. Phase Equilib.*, **14**(3), 400-401 (1993) (Experimental, Phase Diagram, Phase Relations, 5)

[1994Sar] Sari, C., Walker, C.T., Kurata, M., Inoue, T., "Interaction of U-Pu-Zr Alloys Containing Minor Actinides and Rare Earths With Stainless Steel", *J. Nucl. Mater.*, **208**, 201-210 (1994) (Experimental, Morphology, 13)

[1994Kur] Kurata, M., Inoue, T., Sari, C., "Redistribution Behavior of Various Constituents in U-Pu-Zr Alloy and U-Pu-Zr Alloy Containing Minor Actinides and Rare Earths in a Temperature Gradient", *J. Nucl. Mater.*, **208**, 144-158 (1994) (Crys. Structure, Experimental, Phase Diagram, 18)

[1996Kei] Keiser Jr.D.D., Petri, M.C., "Interdiffusion Behavior in U-Pu-Zr Fuel Versus Stainless Steel Couples", *J. Nucl. Mater.*, **240**, 51-61 (1996) (Experimental, Transport Phenomena, 8)

[1997Pet] Petri, M.C., Dayananda, M.A., "Isothermal Diffusion in Uranium-Plutonium-Zirconium Alloys", *J. Nucl. Mater.*, **240**, 131-143 (1997) (Experimental, Transport Phenomena, 25)

[1998Ale] Alekseev, O.A., Smirnov, E.A., Shmakov, A.A., "Interdiffusion in the BCC Phase of the U-Pu-Zr System", *Atom. Ener.*, **84**(4), 260-266 (1998) (Theory, Transport Phenomena, 28)

[1999Kur] Kurata, M., "Thermodynamic Assessment of the Pu-U, Pu-Zr and Pu-U-Zr Systems", *Calphad*, **23**(3-4), 305-337 (1999) (Assessment, Phase Relations, Thermodyn., 12)

[2000Soh] Sohn, Y.H., Dayananda, M.A., Hofman, G.L., Strain, R.V., Hayes, S.L., "Analysis of Constituent Redistribution in the γ (bcc) U-Pu-Zr Alloys Under Gradients of Temperature and Concentrations", *J. Nucl. Mater.*, **279**, 317-329 (2000) (Experimental, Morphology, Transport Phenomena, 42)

[2004Kim] Kim, Y.S., Hofman, G.L., Hayes, S.L., Sohn, Y.H., "Constituent Redistribution in U-Pu-Zr Fuel During Irradiation", *J. Nucl. Mater.*, **327**, 27-36 (2004) (Experimental, Thermodyn., Transport Phenomena, 19)

[2005Nak] Nakamura, K., Ogata, T., Kurata, M., "Analysis of Metal Fuel/Cladding Metallurgical Interaction During Off-Normal Transient Events with Phase Diagram of the U-Pu-Zr-Fe System", *J. Phys. Chem. Solids*, **66**(2-4), 643-646 (2005) (Assessment, Experimental, Phase Diagram, Phase Relations, Thermodyn., 16)

[2005Iiz] Iizuka, M., Kinoshita, K., Koyama, T., "Modeling of Anodic Dissolution of U-Pu-Zr Ternary Alloy in the Molten LiCl-KCl Electrolyte", *J. Phys. Chem. Solids*, **66**(2-4), 427-432 (2005) (Calculation, Interface Phenomena, Kinetics, Phase Relations, 16)

Table 1: Investigations of the Pu-U-Zr Phase Relations, Structures and Thermodynamics

Reference	Method/Experimental Technique	Temperature/Composition/Phase Range Studied
[1966Far1]	not reported	25 - 1150°C, U-29Pu-22.5Zr (at.%) 654 - 1150°C, (γU); 596-654°C, (αU)+(γU); 25-596°C, (αU)+(U,Zr)
[1966Far2]	Dilatometry and DTA	670 - 25°C, U-12.9Pu-22.6Zr (at.%), (αU), (γPu,U,Zr), (U,Zr)
[1967Far2]	Calorimetry	25 - 1150, U-12.2Pu-21.8Zr (at.%) (αU) +(U,Zr); (αU) +(γU)
[1968Tuc]	DTA, optical metallography	Pu-U-Zr, < 865°C, solid solution surface
[1968Far1] [1968Far4]	DTA, optical metallography	< 1000°C, from 100 to 65 at.% Pu, solidus and liquidus surfaces
[1988Lei]	EPMA, optical metallography, DTA, thermodynamic calculations	Solidus and liquidus surfaces
[1990Ger]	not reported	Isothermal sections at 700, 670, and 500°C
[1970Obo]	EMPA, X-ray diffraction, optical metallography	Isothermal sections at 700, 670, 660, 650, 640, 595, 580, 550, and 500°C

Table 2: Crystallographic Data of Solid Phases

Phase/ Temperature Range [°C]	Pearson Symbol/ Space Group/ Prototype	Lattice Parameters [pm]	Comments/References
γ (εPu,γU,βZr) 1855 - 455	*cI*2 *Im*$\bar{3}$*m* W		100%Pu - 100% U - 100% Zr
(εPu) 640 - 463 640 - 455		*a* = 363.8	pure, 500°C, [1989Pet] dissolves 100 at.% U [1989Pet] and 100 at.% Zr in Pu-U system
(γU) 1135 - 776 1135-693		*a* = 352.4	pure, 805°C, [Mas2] dissolves 100 at.% Pu [1989Pet] and 100 at.% Zr in U-Zr system
(βZr) 1855 - 863 1855 - 606		*a* = 360.90	pure, at 863°C [Mas2] in U-Zr system
(δ'Pu) 483 - 463 483 - 442	*tI*2 *I*4/*mmm* In	*a* = 333.9 *c* = 444.6	pure, 477°C, [1989Pet] dissolves 1.3 at.% U at 455°C [1989Pet] and 2 at.% Zr at 463°C [Mas2] in Pu-U system
(δPu) 463 - 320 463 - 280	*cF*4 *Fm*$\bar{3}$*m* Cu	*a* = 463.7	pure, 320°C, [1989Pet] dissolves 0.3 at.% U at 442°C [1989Pet] and 70 at.% Zr at 640-267°C [Mas2] in Pu-Zr system
(γPu) 320 - 215	*oF*8 *Fddd* γPu	*a* = 315.87 *b* = 576.82 *c* = 1016.2	pure, 235°C, [1989Pet] dissolves 0.8 at.% U at 280°C [1989Pet] and 3 at.% Zr at 320-218°C [Mas2]
(βPu) 215 - 125 ~270 - ~115	*mC*34 *C*2/*m* βPu	*a* = 928.4 *b* = 1046.3 *c* = 785.9 β = 92.13°C	pure, 190°C, [1989Pet] dissolves 2.0 at.% U at 280°C [1989Pet] and ~5 at.% Zr at ~260°C [Mas2] in Pu-Zr system
(αPu) < 125	*mP*16 $P2_1/m$ αPu	*a* = 618.3 *b* = 482.2 *c* = 1096.3 β = 101.79°C	pure, 25°C, [1989Pet], the solubilities of U is negligible, dissolves 1.5 at.% Zr at 125°C [Mas2]
(βU) 776 - 560	*tP*30 $P4_2/mnm$ βU	*a* = 1075.9 *c* = 565.6	pure, 720°C, [Mas2] dissolves ~18 at.% Pu at 705°C [1989Pet] and ~2 at.% Zr at 693°C [Mas2]

Phase/ Temperature Range [°C]	Pearson Symbol/ Space Group/ Prototype	Lattice Parameters [pm]	Comments/References
(αU) < 668	*oC*4 *Cmcm* αU	*a* = 285.37 *b* = 586.95 *c* = 495.48	pure, at 25°C [Mas2] dissolves 15 at.% Pu at 560°C [1989Pet], and 0.5 at.% Zr at 668°C [Mas2]
(αZr) < 863	*hP*2 $P6_3/mmm$ Mg	*a* = 323.16 *c* = 514.75	pure, at 25°C [Mas2] dissolves 13 at.% Pu at 863°C [Mas2] and 0.4 at.% U at 863°C [Mas2]
(ωZr)(hp) 25	*hP*2 *P*6/*mmm* ωTi	*a* = 503.6 *c* = 310.9	at 25°C [Mas2] metastable
η, (Pu-U) 705 - 278	*tP*52	 *a* = 1057 *c* = 1076	4 -70 at.% U 25 at.% U at 500°C [1989Pet]
ζ, (Pu-U) < 590	*t***	 *a* = 1069.2 *c/a* ≅ 1 *a* = 1066.4 *c/a* ≅ 1 *a* = 1065.1 *c/a* ≅ 1	25-74 at.% U, dissolves 5 at.% Zr at 25°C, 35 at.% U [1989Pet] at 25°C, 50 at.% U [1989Pet] at 25°C, 70 at.% U [1989Pet]
υ, Pu_4Zr < 345	*tP*80 *P*4/*ncc*	*a* = 1089 *c* = 1489	[VC2]
κ, $PuZr_3$ < 380	*hP*3 *P*6/*mmm* AlB_2	*a* = 506.0 *c* = 311.9	oxygen-stabilized [1967Lau, 1992Zuz]
δ, UZr_2 < 617	*hP*3 *P*6/*mmm* AlB_2	*a* = 503 *c* = 308.0	[1989She] at UZr_2 composition

Table 3: Thermodynamic Data of Reaction or Transformation

Reaction or Transformation	Temperature [°C]	Quantity, per mol of atoms [kJ, mol, K]	Comments
(αU) + (δU,Zr) ⇌ (αU) + (γU)	600 - 650	ΔH = 8.32 kJ·mol^{-1}	Phase transformation, [1967Far2]

Table 4: Thermodynamic Properties of Alloys

Phase	Temperature Range [°C]	Property, per mole of atoms [J, mol, K]	Comments
65.96U-12.23Pu-21.81Zr (at.%)	25 - 600	$\Delta H(T) = -6833.1 + 18.76T + 0.0129\ T^2$ $C_p(T) = 18.76 + 0.0258\ T$	Two phase alloy: (αU) +(U,Zr), [1967Far2]
65.96U-12.23Pu-21.81Zr (at.%)	650 - 1150	$\Delta H(T) = 8560.1 + 14.15T + 0.01265\ T^2$ $C_p(T) = 8.55 + 0.0253\ T$	Two phase alloy: (αU) +(γU), [1967Far2]

Table 5: Investigations of the Pu-U-Zr Materials Properties

Reference	Method/Experimental Technique	Type of Property
[1965Far]	Dilatometry	Temperature expansion coefficient at temperatures from 25 to 950°C
[1966Far1]	Thermoconductivity	Thermoconductivity coefficient at temperatures from 100 to 900°C
[1966Far2]	Mechanical properties, compressive and tensile tests at room and high temperatures, creep	Ultimate compressive strength, Yield tensile strength, Ultimate tensile strength, Young's modulus, Time, min, to attain 2% strain
[1967Far1]	Neutron radiography, optical metallography	Elongation and porosity after irradiation
[1967Far2]	Calorimetry	Heat content, specific heat, solid state heat of transformation
[1969Rhu]	Microprobe scan, optical metallography	Redistribution of elements in cross section of fuel-pin under irradiation
[1990Por]	Optical metallography, neutron radiography, isotopic dilution mass spectrometry, spectophotometric analysis	Fuel constituent redistribution, fuel swelling
[1990Pah]	Optical metallography, EMPA, neutron radiography, immersion density	Fuel constituent redistribution, fuel swelling, fission gas retention and release, fuel/cladding chemical interaction
[1990Ger]	Optical metallography, scanning electron microscopy employing secondary electron microscopy and backscattered electron detection.	Fuel pin swelling
[1993Cra]	Neutron radiography, contact profilometry, Gamma scan, fission gas analysis, optical metallography	Axial growth under irradiation, fuel-cladding chemical interaction
[1994Kur]	Optical metallography, α-autoradiography, EMPA	Fuel-cladding chemical interaction
[1994Sar]	Optical metallography, EMPA, dilatometry	Fuel-cladding chemical interaction
[1996Kei]	Diffusion couples, SEM/EDX analysis	Interdiffusion behavior in Pu-U-Zr fuel versus stainless steel

Reference	Method/Experimental Technique	Type of Property
[1997Pet]	Diffusion couples, SEM/EDX analysis, mass spectrometry	Isothermal diffusion in Pu-U-Zr alloys
[1998Ale]	Diffusion couples, X-ray microanalysis	Interdiffusion in the BCC phase of the Pu-U-Zr system
[2000Soh]	SEM, EMPA, scanning Auge microscopy	Constituent redistribution under gradients temperature and concentrations
[2004Kim]	Optical microscopy, SEM, EMPA	Constituent redistribution during irradiation

Table 6: Ultimate Compressive Strength of Pu-U-Zr Alloys at Selected Temperatures

Alloy composition (at.%)	Heat-treatment	Ultimate Compressive Strength at Indicated Temperature [MPa]				
		25°C	500°C	625°C	675°C	750°C
U-9.5Pu-14.4Zr	Hom.*	1608.84		117.72	39.24	
U-9.5Pu-29.2Zr	Hom.	1628.46			67.69	41.20
	As cast	1608.84	>539.55	117.72	51.01	
U-12.2Pu-21.8Zr	As cast	1245.87	539.55	107.91	24.53	
U-14.2Pu-14.5Zr	As cast	1265.49	470.88	107.91	54.94	
U-14.4Pu-29.3Zr	Hom.	1137.96			54.94	

* Homogenizing heat-treatment: 1050°C for one week, oil quench for the alloys with more than 22 at.% Zr; and 950°C for one week, oil quench for the alloys with less than 22 at.% Zr

Table 7: Variations of Tensile Properties with Temperature in Homogenized and Quenched* Uranium-Plutonium-Zirconium Alloys

Alloy, at.%	*T* [°C]	Tensile strength		Yong's modulus (E) [GPa]	Type failure
		Ultimate [MPa]	Yield** [MPa]		
U-9.5Pu-14.4Zr	25	177.56		170.69	Brittle
	675	11.77	10.79	13.73	Ductile
U-14.2Pu-14.5Zr	25	39.24		103.99	Brittle
	675	11.77	10.79	15.70	Ductile
U-14.4Pu-29.5Zr	25	75.54		127.53	Brittle
	675	28.45	27.47	18.64	Ductile

* All specimens were tested in creep prior the tensile tests and therefore contain some (<5%) hot work.
** Yield strength at 0.2% offset. Brittle specimens did not attain this before fracturing

Table 8: Time (min) To Attain 2% Strain in Pu-U-Zr Alloys

Alloy composition (at.%)	Load [MPa]	Temperature [°C]				
		600	625	650	675	700
U-9.5Pu-14.4Zr	4.91				15	
	9.81				5	
	19.62				3	
	39.24		5		1	
U-14.2Pu-14.5Zr	4.91				10	
	9.81		5.000		1	
	19.62		210			
	39.24		10			
U-12.2Pu-21.8Zr	4.91			5.000		
	9.81		5.000	80		
	19.62		210	1		
	39.24		10			
U-14.4Pu-29.5Zr	4.91	100.000		5.000	45	40
	9.81	10.000		80	5	5
	19.62	800		1	1	1
	39.24	70				

Table 9: Key Phenomena that Control Fuel Performance

Phenomena	Experimental Observations	Consequences
Fuel swelling	irradiation growth and grain boundary tearing; Xe/Kr bubble growth; solid fission product accumulation; alloy and burnup rate effects	reactivity loss; rate of gas release; fiel/clad interaction stresses; thermal conductivity loss
Fuel constituent migration	U/Zr interdiffusion; critical Pu threshold	lowered solidus; complexities of properties modeling
Fuel/cladding chemical interaction	penetration into cladding by U, Pu, and lanthanide series fission products; diffusion of cladding constituents into fuel; extensive nickel loss in austenitics	cladding wall thinning; ductility degradation of interaction layer in cladding; eutectic composition approached in fuel
Cladding deformation	irradiation/thermal creep by fission gas pressure loading; some fuel contact pressure loading; void swelling in austenitics	stress-rupture lifetime determines ultimate burnup achieved; high cladding strains can lead to element/bundle interaction stresses

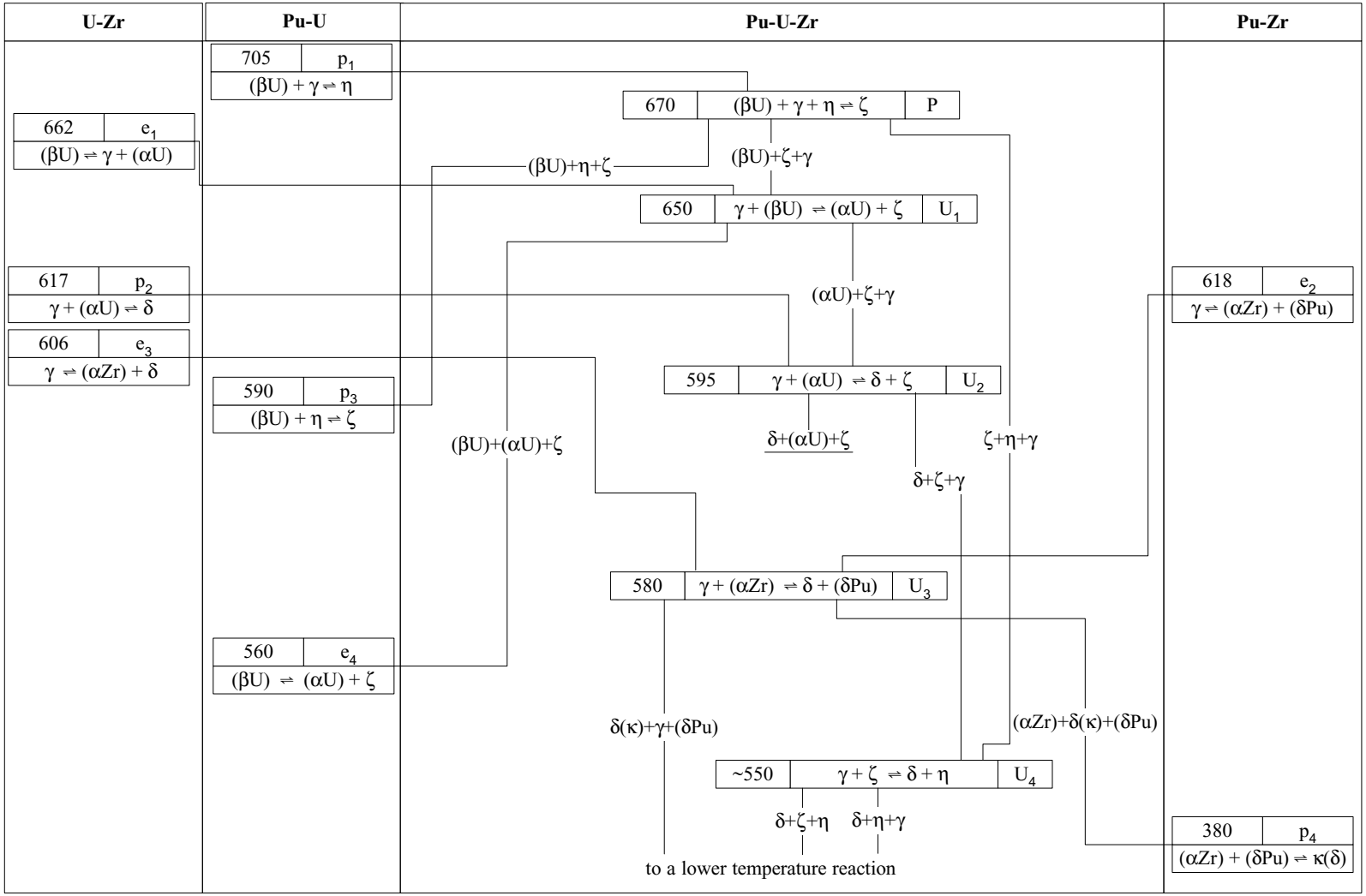

Fig. 1: Pu-U-Zr. Partial reaction scheme

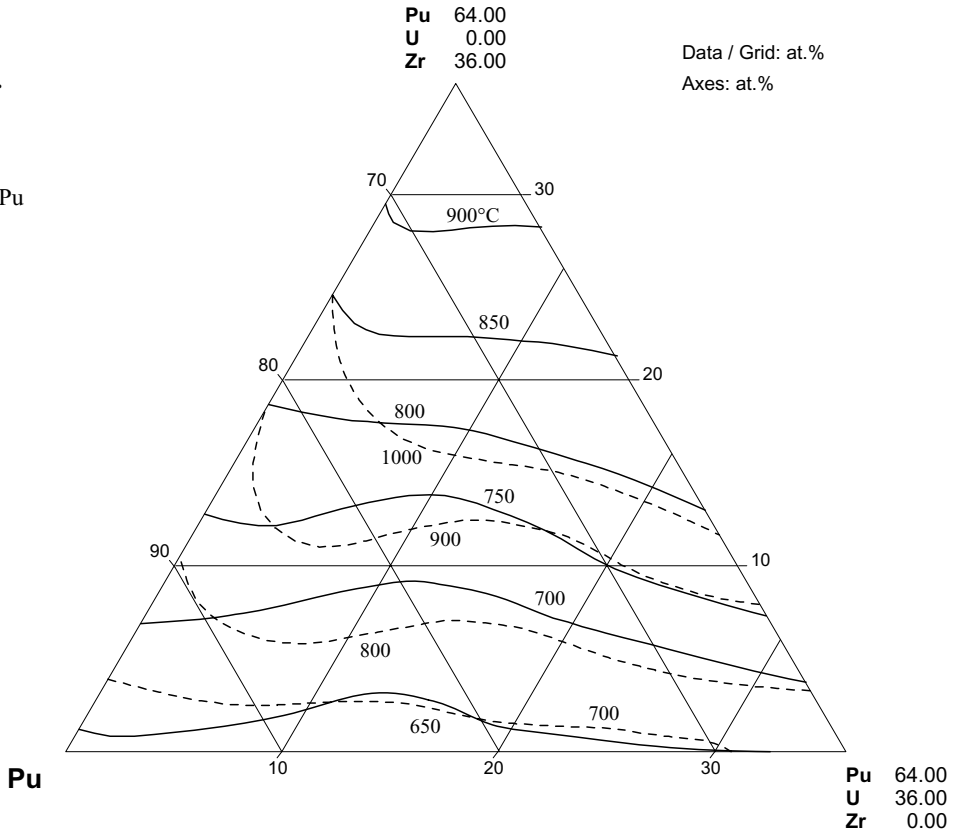

Fig. 2: Pu-U-Zr. Liquidus (dashed lines) and solidus (solid lines) temperature in the Pu rich corner

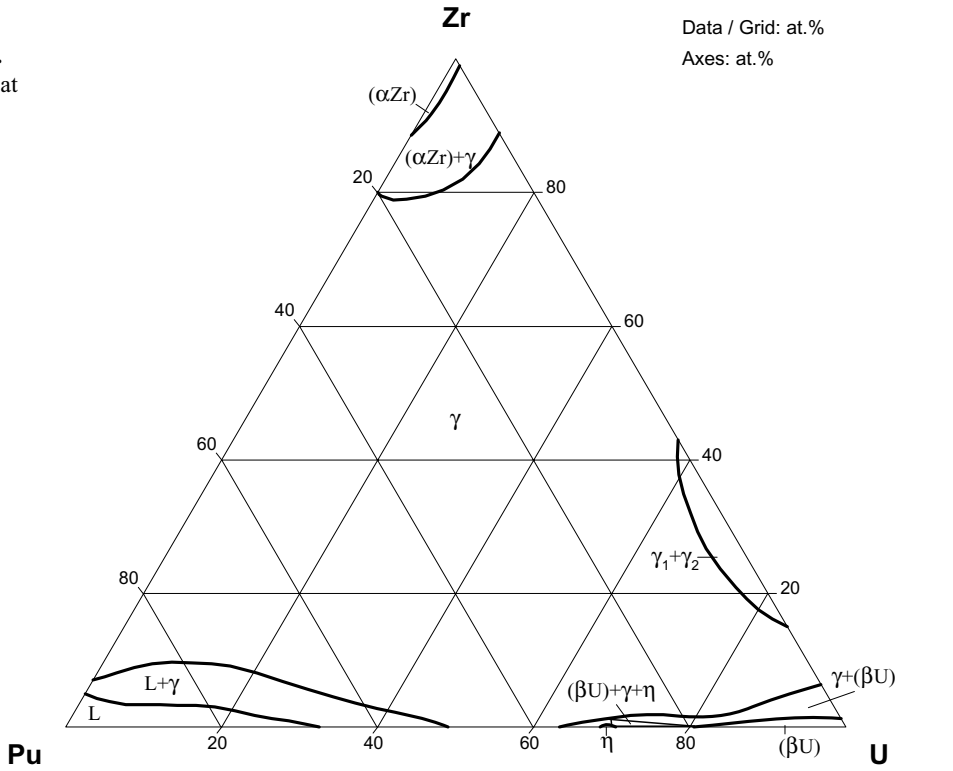

Fig. 3: Pu-U-Zr. Isothermal section at 700°C

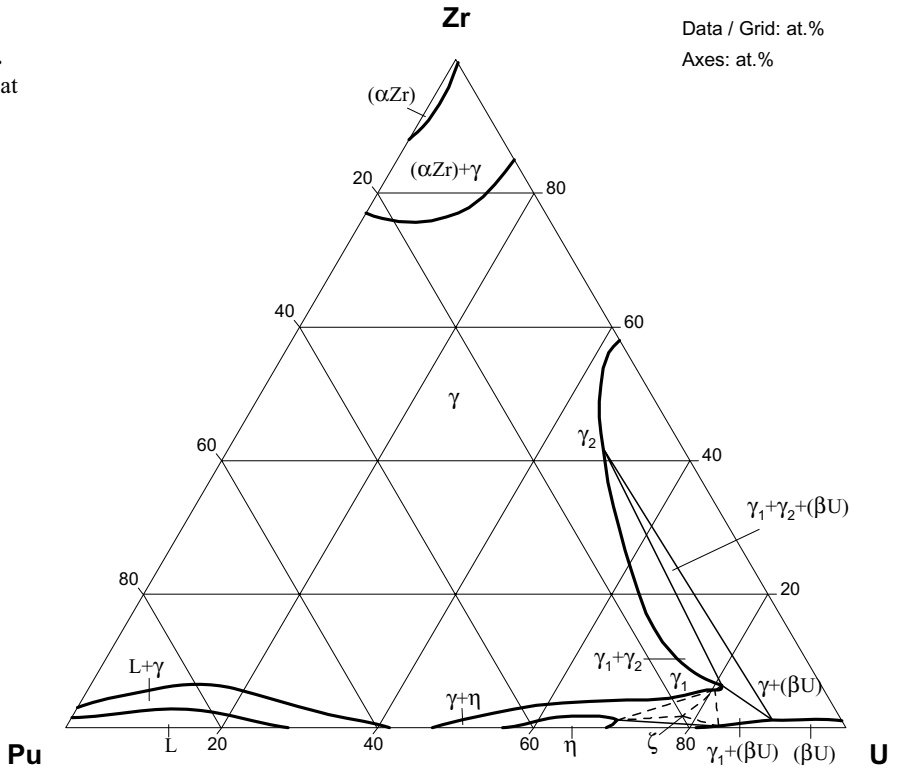

Fig. 4: Pu-U-Zr. Isothermal section at 670°C

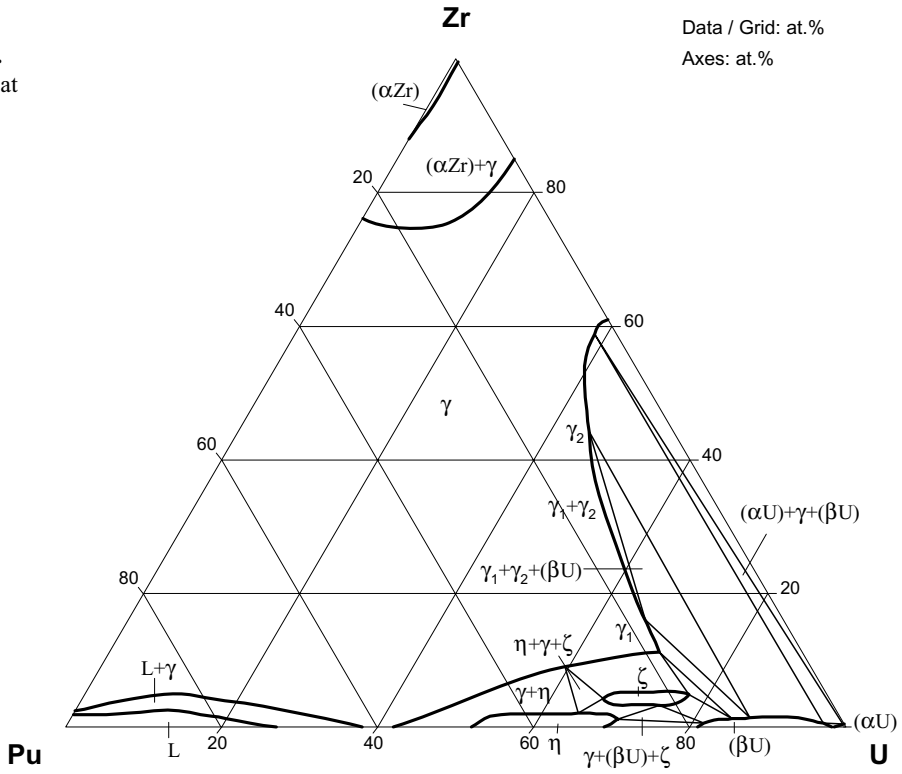

Fig. 5: Pu-U-Zr. Isothermal section at 660°C

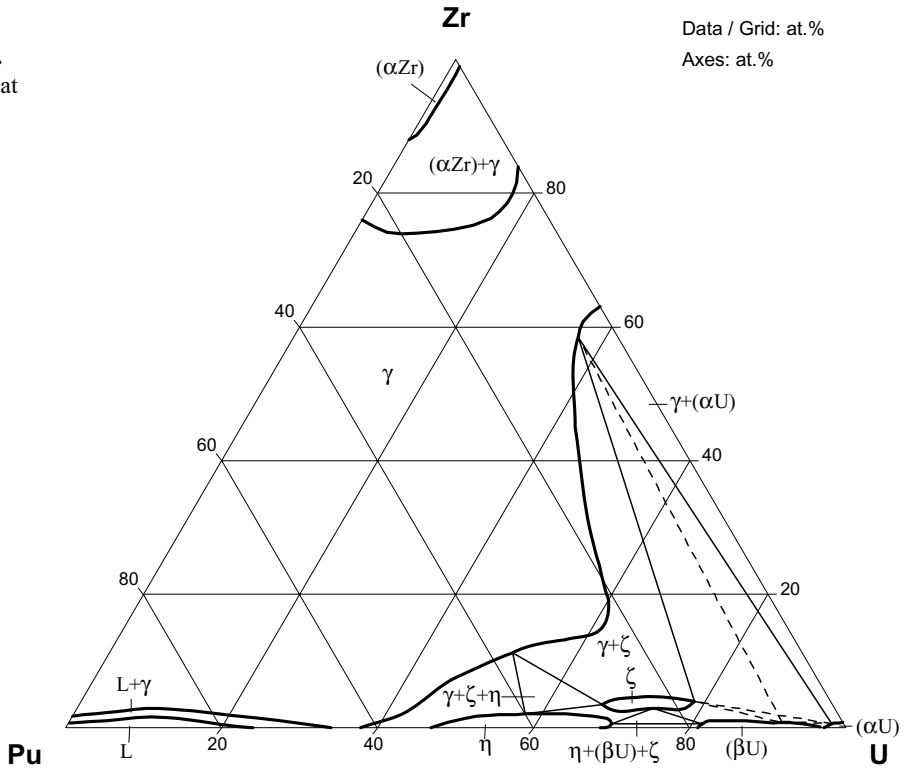

Fig. 6: Pu-U-Zr. Isothermal section at 650°C

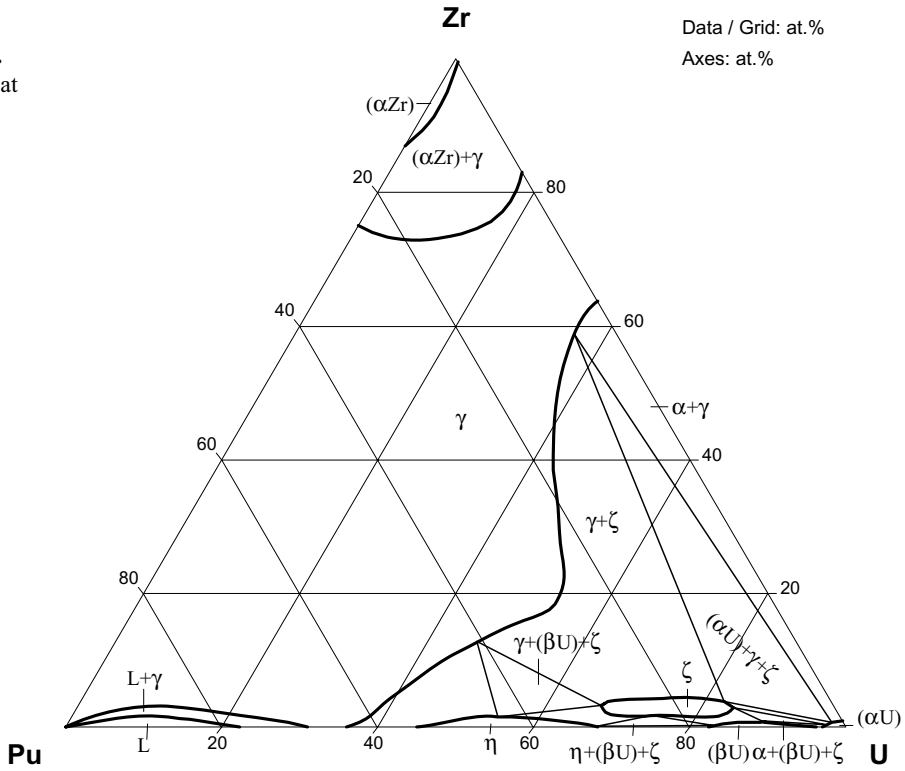

Fig. 7: Pu-U-Zr. Isothermal section at 640°C

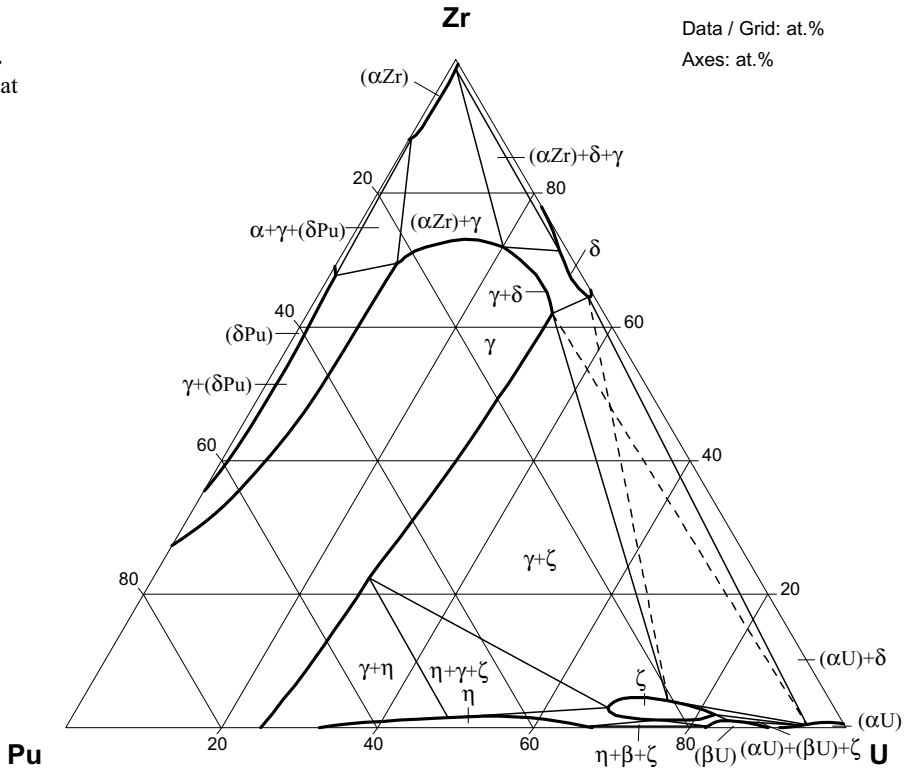

Fig. 8: Pu-U-Zr. Isothermal section at 595°C

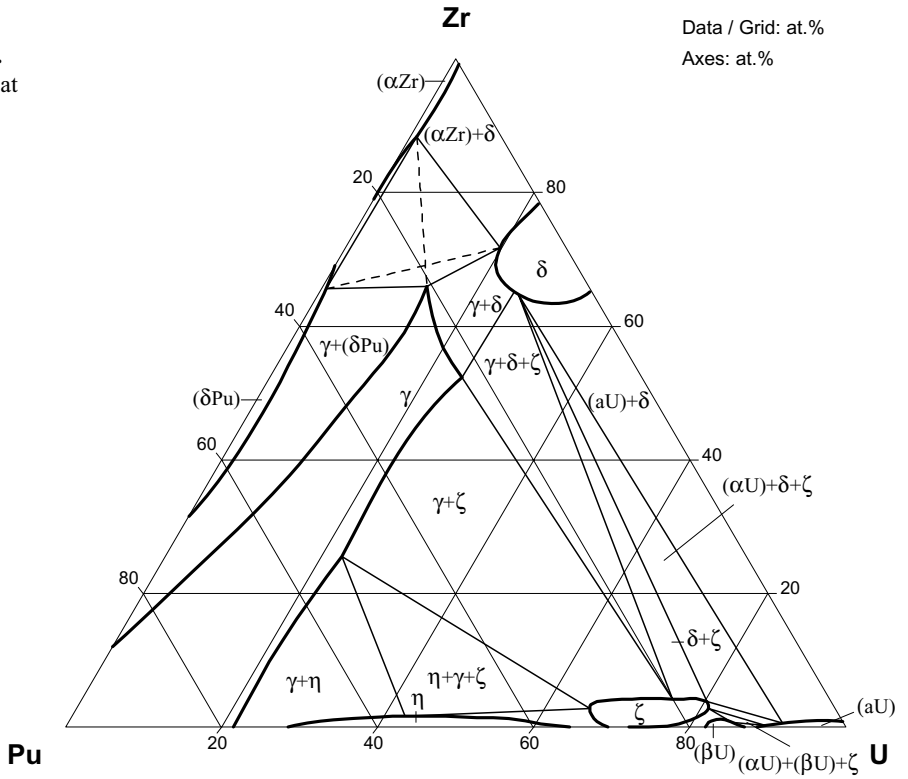

Fig. 9: Pu-U-Zr. Isothermal section at 580°C

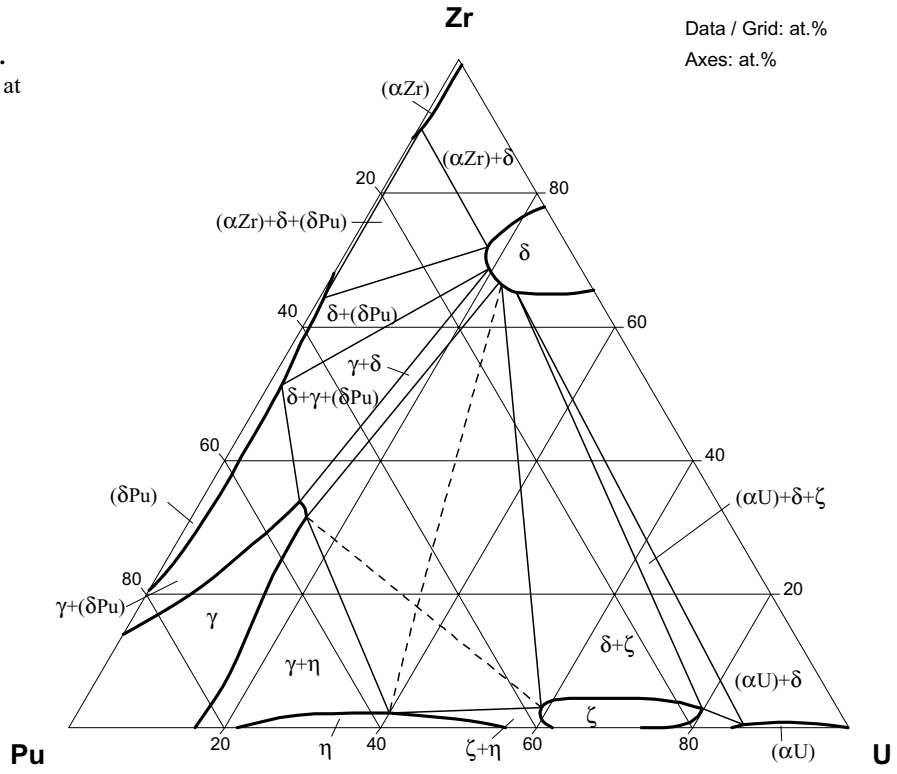

Fig. 10: Pu-U-Zr. Isothermal section at 550°C

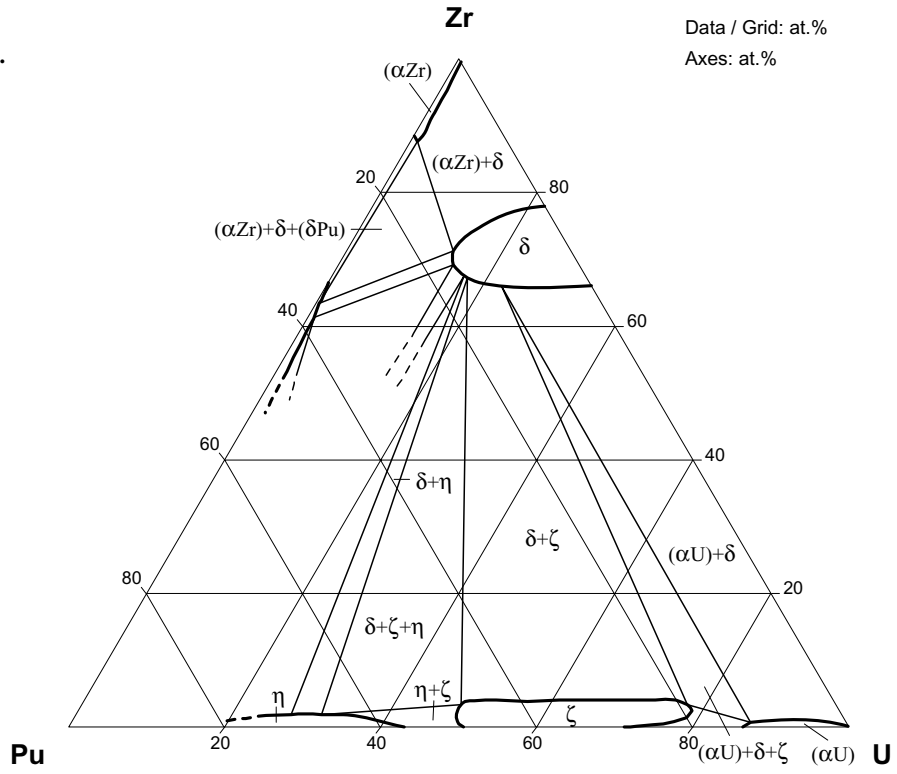

Fig. 11: Pu-U-Zr. Partial isothermal section at 500°C